*J. Fluid Mech.* (1967), *vol.* 30, *part* 2, *pp.* 285–303
*Printed in Great Britain*



# The nozzle-fluid concentration field of the round, turbulent, free jet

By H. A. BECKER,† H. C. HOTTEL AND G. C. WILLIAMS
Department of Chemical Engineering, Massachusetts Institute of Technology

(Received 6 September 1966)

The light-scatter technique has been used to study the nozzle-fluid concentration field in an isothermal, turbulent, axisymmetric air/air free jet with the nozzle air marked by an oil smoke. The data on the mean concentration field appear to be the most accurate yet obtained, due to the peculiar advantages of the technique. The turbulent concentration fluctuations have been characterized as to intensity, spectral distribution, and two-point correlation. The intermittency factor has been measured and the properties of the turbulent fluid computed. Comparison with the results of other investigators who used heat to mark the nozzle fluid indicates a close similarity between the concentration and temperature fields.

## 1. Introduction

The field of mean concentration or temperature due to the spreading of the source fluid in a free turbulent jet discharging into a stagnant atmosphere has been mapped many times. Corrsin & Uberoi (1950, 1951) used the hot-wire anemometer to detect temperature fluctuations. Concentration fluctuations were first characterized by Rosensweig, Hottel & Williams (1961) in a study of the feasibility of using light scatter to follow the process of turbulent mixing between several fluid streams, one of which is marked with colloidal particles. This technique has been improved (Becker, Hottel & Williams 1967, referred to below as I) and the present paper reports results on the free jet which are as good as the technique is easily capable of giving. The concentration field of a sol marking the jet source-fluid was studied as to mean value, fluctuation intensity, scale, and intermittency. Because of the unique advantages of scattered-light detection for the *in situ* investigation of concentration fields, such as linear response, non-disturbance of the flow field, rapidity of execution, etc., these data afford a more accurate description of most aspects of the source-fluid concentration field than can be obtained by any other means currently available. Interpretation of the concentration field in relation to a comparably accurate picture of the velocity field awaits results of investigations now in progress.

† Present address: Department of Chemical Engineering, Queen's University, Kingston, Ontario, Canada.

## 2. Apparatus and methods

The jet was of air discharging into stagnant room air, with negligible temperature variation, from an essentially ideal flow nozzle of 0·635 cm throat diameter and 2·41 cm upstream tube diameter. The nozzle air was marked with an oil smoke. Most of the experiments were carried out at a nozzle air velocity of 130 m/sec, giving a nozzle Reynolds number of 54,000.

The principle of the light-scatter technique has been described in other publications (Rosensweig 1959; Rosensweig *et al.* 1961; Becker 1961; and Becker, Hottel & Williams 1963). The limitations of the technique and the corrections for finite probe size, noise, and other sources of error have been determined (Becker, Hottel & Williams 1967). These corrections were applied to the present data.

A true root-mean-square voltmeter (Flow Corporation Model 12A1), a correlation amplifier (Flow Corporation Model 13A1), and a sound analyzer (General Radio Model 1564A) were used for the analysis of concentration fluctuations. The system used for the study of intermittency has been described elsewhere (Becker, Hottel & Williams 1965). Instruments used for turbulence measurements were calibrated on random noise.

## 3. The mean concentration

The Schmidt number of the marker (oil smoke) particles in air was about 38,000. In respect to its mean concentration field this smoke therefore portrays the case of a Schmidt number on the order of or greater than unity, in which case molecular diffusion in the turbulent jet is insignificant relative to turbulent transport. The ratio between the local mean smoke concentration and the nozzle concentration, $\overline{\Gamma}/\Gamma_0$, may consequently be equated with the volume fraction of nozzle fluid, the mixing process being isopycnic.

The radial profiles of the mean concentration at various axial positions $x$ were faired on graphs of $\ln[\ln(\overline{\Gamma}/\overline{\Gamma}_c)]$ *vs* $\ln[r^2]$ and $\ln[\overline{\Gamma}/\overline{\Gamma}_c]$ *vs.* $r^2$, where $\overline{\Gamma}_c$ is the centreline ($r = 0$) value of the mean concentration $\overline{\Gamma}$ and $r$ is the radial coordinate in a cylindrical frame with $Ox$ at the nozzle mouth. Let the radial positions characterized by constant values of the reduced concentration $\overline{\Gamma}/\overline{\Gamma}_c \equiv \overline{\Gamma}(x,r)/\overline{\Gamma}(x,0)$ be denoted by $b$,

$$b \equiv b(x,\overline{\Gamma}/\overline{\Gamma}_c).$$

The radial profile of the mean concentration was found to become self-preserving, to the accuracy of the data, about 40 nozzle radii downstream of the nozzle: further downstream the characteristic radii $b$ are linear functions of $x$ regressing on a common virtual origin for all values of $\overline{\Gamma}/\overline{\Gamma}_c$, and the centre line concentration $\overline{\Gamma}_c$ varies inversely with the distance from this origin. These relationships are illustrated in figure 1 in which the regression law of the concentration 'half-radius' $b_{\frac{1}{2}} \equiv b(x, \frac{1}{2})$ is

$$b_{\frac{1}{2}} = 0{\cdot}106\,[x - 4{\cdot}8r_0], \tag{1}$$

while the decay law of the centreline concentration is

$$\Gamma_0/\overline{\Gamma}_c = 0{\cdot}0925\,[x - 4{\cdot}8r_0]/r_0, \tag{2}$$

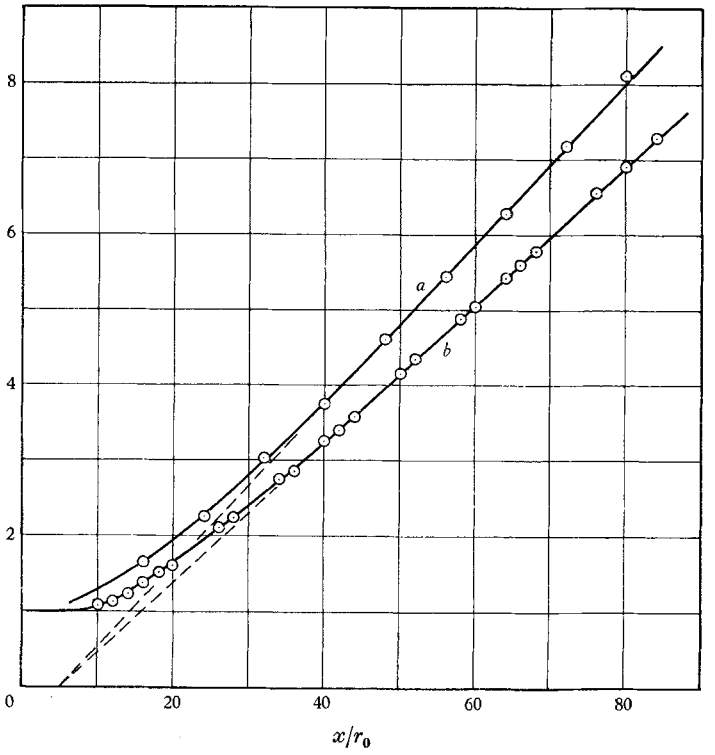


FIGURE 1. The normalized concentration half-radius $b_{\frac{1}{2}}/r_0$ (curve *a*) and the reciprocal $\Gamma_0/\overline{\Gamma}_c$ (curve *b*) of the normalized centre line mean concentration as functions of distance from the nozzle.

| $\overline{\Gamma}/\overline{\Gamma}_c$ | $\eta$ | $r/b_{\frac{1}{2}}$ | $\bar{\delta}$ | $\gamma'/\gamma'_c$ | $\overline{\Gamma}_T/\overline{\Gamma}_c$ | $\gamma'_T/\overline{\Gamma}_T$ |
|---|---|---|---|---|---|---|
| 1 | 0 | 0 | 1 | 1 | 1 | 0·222 |
| 0·9 | 0·0421 | 0·397 | 1·000 | 1·083 | 0·900 | 0·268 |
| 0·8 | 0·0600 | 0·566 | 1·000 | 1·125 | 0·800 | 0·313 |
| 0·7 | 0·0757 | 0·714 | 1·000 | 1·145 | 0·700 | 0·365 |
| 0·6 | 0·0911 | 0·860 | 1·000 | 1·148 | 0·600 | 0·427 |
| 0·5 | 0·1060 | 1·000 | 0·997 | 1·123 | 0·502 | 0·497 |
| 0·4 | 0·1222 | 1·153 | 0·986 | 1·070 | 0·406 | 0·581 |
| 0·3 | 0·1408 | 1·328 | 0·944 | 0·960 | 0·318 | 0·651 |
| 0·2 | 0·1616 | 1·523 | 0·818 | 0·820 | 0·244 | 0·708 |
| 0·15 | 0·1733 | 1·633 | 0·704 | 0·730 | 0·213 | 0·722 |
| 0·1 | 0·1865 | 1·758 | 0·537 | 0·608 | 0·186 | 0·732 |
| 0·07 | 0·1966 | 1·853 | 0·408 | 0·522 | 0·171 | 0·732 |
| 0·04 | 0·2099 | 1·981 | 0·264 | 0·415 | 0·153 | 0·820 |
| 0·02 | 0·2270 | 2·141 | 0·136 | 0·287 | 0·147 | 0·742 |
| 0·01 | 0·2415 | 2·276 | 0·073 | 0·193 | 0·136 | 0·646 |
| 0·0033 | 0·2640 | 2·490 | 0·026 | — | 0·127 | — |
| — | 0·2800 | 2·640 | 0·012 | — | — | — |

TABLE 1. Numerical specification of the self-preserving profiles of the mean concentration, the concentration fluctuation intensity, and the intermittency factor.

where $r_0$ is the nozzle radius and $\Gamma_0$ the nozzle concentration. The values of $b/[x-4{\cdot}8r_0]$ for a series of values of $\overline{\Gamma}/\overline{\Gamma}_c$ (namely $0{\cdot}9, 0{\cdot}8, \ldots, 0{\cdot}01, 0{\cdot}0033$) were therefore averaged for the profiles downstream of $x = 40r_0$ and give a statistically unbiased estimate of the self-preserving form

$$\overline{\Gamma}/\overline{\Gamma}_c = f(\eta),$$

where $\eta \equiv r/(x-x_0)$ with, in the present jet, $x_0 = 4{\cdot}8r_0$. The numerical results are summarized in table 1.

The mean concentration at a given section $x$ was well-defined at levels above $0{\cdot}005\overline{\Gamma}_c$; at lower levels the low-frequency fluctuations associated with intermittency introduced considerable uncertainty (the largest averaging time used

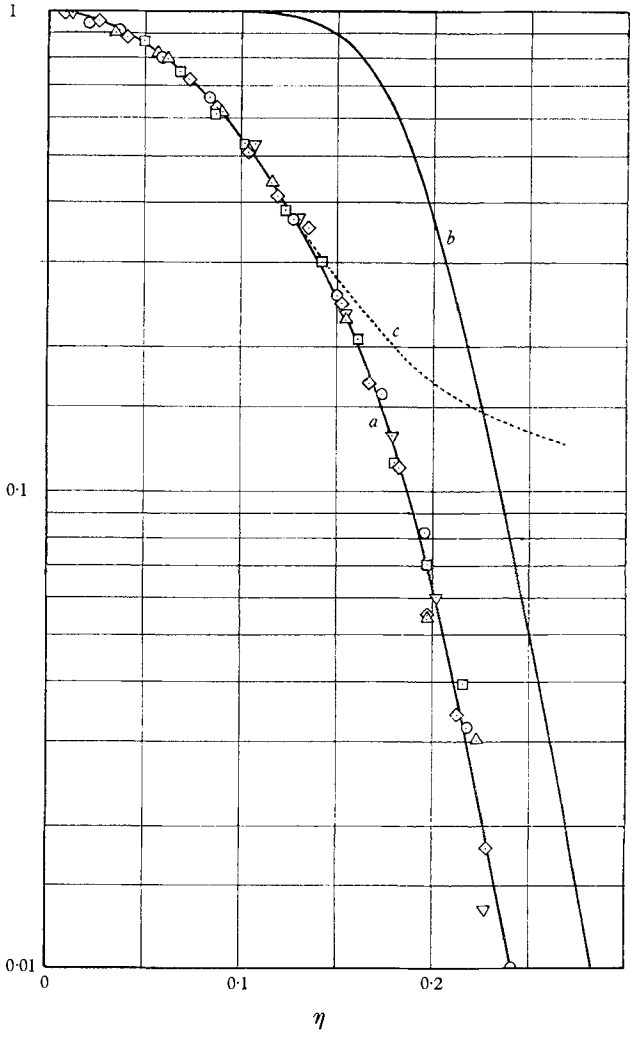


FIGURE 2. The normalized self-preserving radial profiles of the mean concentration $\overline{\Gamma}/\overline{\Gamma}_c$ (curve *a*), the intermittency factor $\bar{\delta}$ (curve *b*), and the mean concentration in the turbulent fluid $\overline{\Gamma}_T/\overline{\Gamma}_c \equiv \overline{\Gamma}/\bar{\delta}\overline{\Gamma}_c$ (curve *c*). The mean concentration data are for axial positions $x/r_0$: ○, 40; □, 48; ◇, 56; △, 64; ▽, 72.

for the mean concentration measurement was 30 sec). The core of the self-preserving profile numerically specified in table 1 is accurately described by the Gaussian-type function

$$\overline{\Gamma} = \overline{\Gamma}_c \exp\{-61{\cdot}6\eta^2\}, \tag{3}$$

where $\eta < 0{\cdot}125$ or $\overline{\Gamma} > 0{\cdot}4\overline{\Gamma}_c$ (the maximum discrepancy in $\overline{\Gamma}/\overline{\Gamma}_c$ is $\pm 0{\cdot}003$, which is just within the probable error of the faired data). This function remains fairly accurate up to $\eta = 0{\cdot}165$ or $\overline{\Gamma} = 0{\cdot}18\overline{\Gamma}_c$, $\overline{\Gamma}/\overline{\Gamma}_c$ agreeing with table 1 within 0·005. The outer domain $0{\cdot}19 < \eta < 0{\cdot}26$, or $0{\cdot}08 > \overline{\Gamma}/\overline{\Gamma}_c > 0{\cdot}004$, which extends to the limit of the region investigated, is well described by

$$\overline{\Gamma} = 2{\cdot}93\overline{\Gamma}_c \exp\{-97\eta^2\}. \tag{4}$$

Figure 2 juxtaposes some of the primary data and the faired curve given by table 1.

## 4. Intermittency

The nozzle fluid pervades the turbulent fluid inside the instantaneous jet boundary but, if the Schmidt number is large, is absent outside it. Thus it is only necessary to convert the instantaneous concentration signal $\Gamma$ into a step function

$$\delta = 1, \quad \Gamma > 0; \quad \delta = 0, \quad \Gamma = 0$$

and time-average the result in order to obtain the intermittency factor $\overline{\delta}$,

$$\overline{\delta} \equiv \text{prob}\{\Gamma > 0\}.$$

The details of this measurement are given in our 1965 paper.

Corrsin & Kistler (1955) pointed out that if the instantaneous boundary of a free turbulent flow is so little convoluted that at given co-ordinates $(x, \phi)$ its radial position is uniquely defined, then

$$\overline{\delta} = \text{prob}\{R > r\},$$

where $R$ is the instantaneous jet radius at $(x, \phi)$. Again,

$$\overline{\delta} = 1 - F(r),$$

where $F(r)$ is the probability distribution function of $R$. Corrsin & Kistler found the distribution of $R$ in a free jet to be nearly random, based on measurements with a hot-wire anemometer. The present data were therefore analysed by means of Gaussian probability graphs, one of which is shown in figure 3. The relationship is linear in the range $0{\cdot}15 < \overline{\delta} < 0{\cdot}95$. The equation of the linear region is

$$\overline{\delta} = \tfrac{1}{2}\,\text{erfc}\left\{\frac{r-\bar{R}}{\sqrt{2}\,\sigma}\right\}, \tag{5}$$

where $\bar{R}$ is the mean radius of the turbulent jet,

$$R = \bar{R} \quad \text{at} \quad \overline{\delta} = \tfrac{1}{2},$$

and, to a fair approximation, $\sigma$ is the standard deviation of the instantaneous radius from the mean,

$$\sigma \simeq \overline{(R-\bar{R})^2}.$$

Intermittency profiles were obtained at $x/r_0 = 32$, 48 and 64. The profiles at $x/r_0 = 48$ and 64 indicate the reasonable result that the mean jet radius $\bar{R}$ regresses on a common virtual origin with the mean-concentration radii $b$, giving

$$\bar{R} = 0{\cdot}189\,[x - 4{\cdot}8r_0]. \tag{6}$$

The 'wrinkle amplitude' $\sigma$, on the other hand, appears to regress on about the same virtual origin as the integral spatial scale of the concentration fluctuations (see § 6), giving

$$\sigma = 0{\cdot}0305x. \tag{7}$$

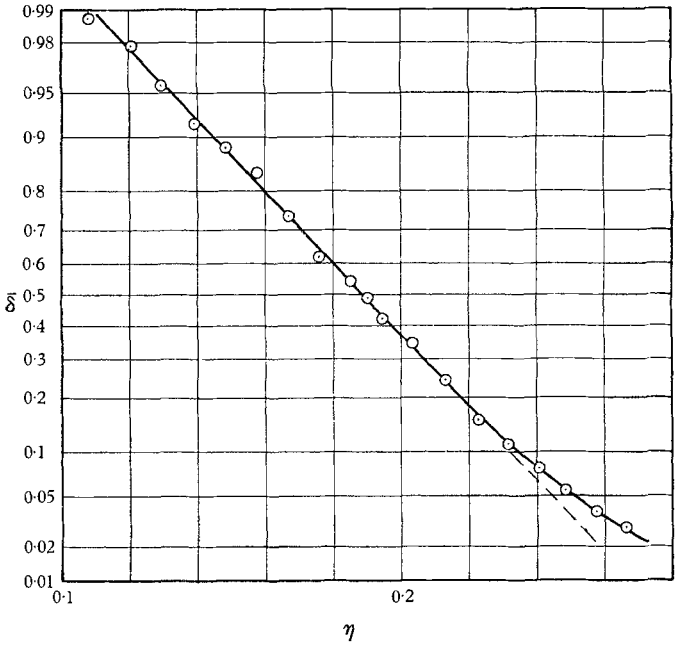


FIGURE 3. The radial profile of the intermittency factor at $x = 48r_0$, on probability paper.

The difference in the virtual origins of $\bar{R}$ and $\sigma$ visibly affects the intermittency profiles at $x/r_0 = 48$ and 64 only at $\bar{\delta} > 0{\cdot}4$. Thus, for the final estimate of the self-preserving form of the intermittency profile, (5) has been taken to apply at $\bar{\delta} > 0{\cdot}3$, with $\bar{R}$ given by (6) and $\sigma$ by (7), while at $\bar{\delta} < 0{\cdot}3$ the profile is given directly by the faired experimental data. The resulting specification of the self-preserving profile is given in table 1. Figure 4 shows the experimental data juxtaposed with the self-preserving form.

The data considered in this section were presented earlier in our 1965 paper on intermittency in jets, but the primary interest then was in the behaviour of the round jet confined by a cylindrical enclosure. It was concluded that in the free jet the mean radius $\bar{R}$ and the concentration half-radius $b_{\frac{1}{2}}$ are related by

$$\bar{R} = 1{\cdot}57b_{\frac{1}{2}} + 0{\cdot}8r_0.$$

The present more critical analysis of the mean concentration and intermittency profiles, however, fails to support a distinction between the virtual origins of $\bar{R}$

and $b_{\frac{1}{2}}$, and the self-preserving relation between these parameters appears to be simply

$$\bar{R} = 1{\cdot}78 b_{\frac{1}{2}}. \tag{8}$$

A compounding of small inaccuracies led to the erroneous earlier result.

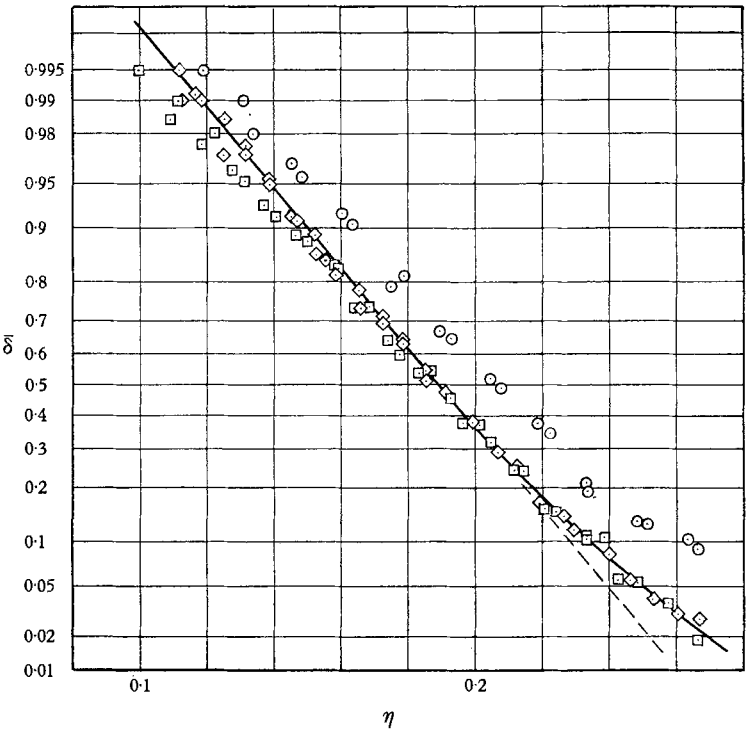


FIGURE 4. Radial profiles of the intermittency factor. The curve represents the estimate of the self-preserving form. The data are for axial positions $x/r_0$: ○, 32; □, 48; ◇, 64.

## 5. The intensity of concentration fluctuations

The scattered-light technique cannot discriminate the *total* mean-square fluctuation in the concentration of marker sol: owing to the very slow particle diffusion (with correspondingly large particle Schmidt number) a considerable portion of the fluctuation energy lies in concentration eddies too small to see with the smallest feasible probe (see I). However, it is not difficult with electronic filters and a suitable choice of probe diameter to arrange that the high-frequency cutoff occurs within the $-\frac{5}{3}$ power (or equivalent) region of the spectrum. A correction on spatial resolution may then be applied as described in I which transforms the measured mean-square signal fluctuation into the concentration fluctuation obtaining if the $-\frac{5}{3}$ or equivalent power law held at wave-numbers up to infinity. This correction is normally less than 5 %. The result is a mean-square fluctuation value $\overline{\gamma^2}$ appropriate to a Schmidt number on the order of unity, which is the normal case in gas mixing. Thus the present values of $\overline{\gamma^2}$ so arrived at for air–air jet mixing with an oil–smoke nozzle-air marker effectively represent the mean-square fluctuation in the concentration of nozzle gas in constant-density gas jet mixing.

The root-mean-square concentration fluctuation $\sqrt{\overline{\gamma^2}}$ is called the concentration fluctuation *intensity* and denoted by $\gamma'$. The radial profiles of the intensity normalized with respect to the centre line intensity $\gamma'_c$ were found to have the same virtual origin as the mean concentration. Figure 5 therefore shows the intensity profile in the appropriate form

$$\gamma'/\gamma'_0 = f(\eta),$$

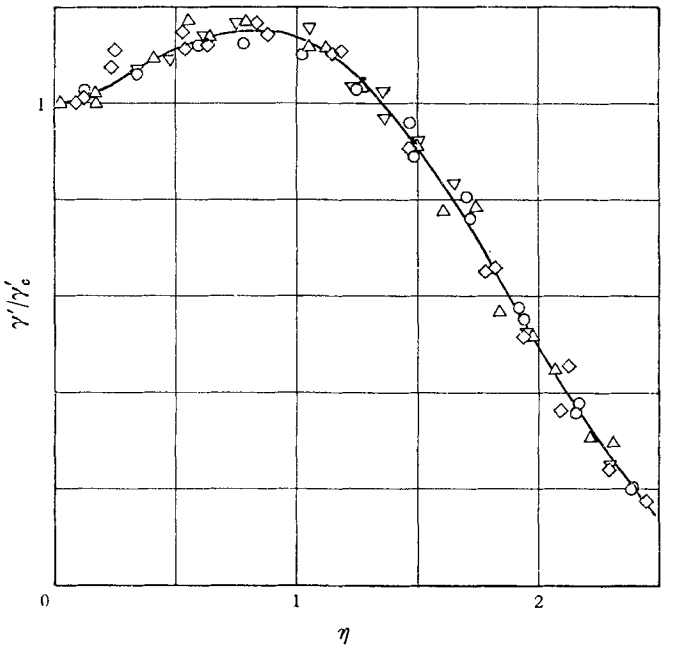


FIGURE 5. The radial profile of the concentration fluctuation intensity. The curve represents the estimate of the self-preserving form. The data are for axial positions $x/r_0$: ○, 40; □, 48; ◇, 56; △, 64; ▽, 72.

where $\eta \equiv r/(x-4{\cdot}8r_0)$. A numerical specification of the self-preserving profile (the curve through the data in figure 5) is given in table 1.

Figure 6 shows the intensity as a function of position on the jet centre line. The jet source was of uniform discharge velocity and the concentration fluctuations accordingly begin at the tip of the initial core region of uniform flow—the 'potential cone'—about 8 nozzle radii downstream of the nozzle mouth. Between 8 and 17 nozzle radii downstream the intensity climbs rapidly to a first maximum at which the basic structure of the turbulent jet may be considered as formed but not yet in equilibrium. There then ensues an asymptotic approach to the equilibrium value characteristic of the ultimate self preserving state. For the estimation of this equilibrium value a graph of $\Gamma_0/\gamma'_c$ *vs.* $\Gamma_0/\overline{\Gamma}_c$ is appropriate and is shown in figure 7. The equation of the linear region is

$$\frac{\gamma'_c}{\overline{\Gamma}_c} = \frac{0{\cdot}222}{1+0{\cdot}6\overline{\Gamma}_c/\Gamma_0}, \tag{9}$$

which indicates that in self-preservation $\gamma'_c = 0{\cdot}222\overline{\Gamma}_c$.

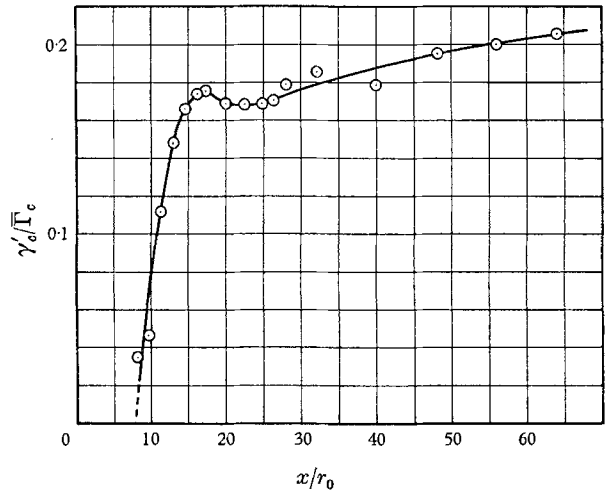


FIGURE 6. The relative concentration fluctuation intensity on the jet centre line as a function of distance from the nozzle.

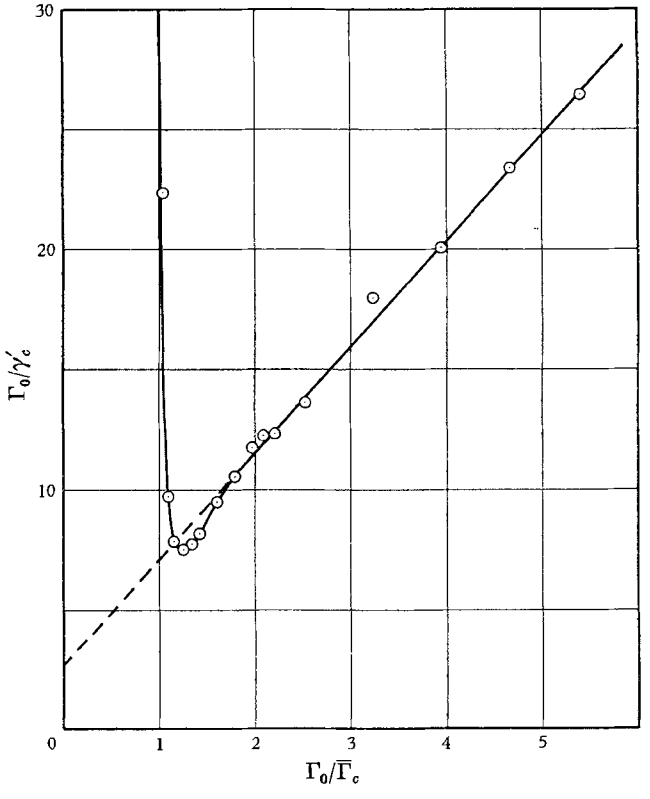


FIGURE 7. The reciprocal of the concentration fluctuation intensity as a function of the reciprocal of the mean concentration along the jet centre line.

It is interesting to examine the self-preserving relation between the mean-square concentration fluctuation $\overline{\gamma^2}$ and the mean concentration $\overline{\Gamma}$. If the instantaneous concentration $\Gamma$ simply fluctuated between zero and a fixed value $\Gamma_1$ we would have

$$\begin{aligned}\overline{\gamma^2} &= (\Gamma_1-\overline{\Gamma})\,\overline{\delta}+\overline{\Gamma}(1-\overline{\delta})\\ &= (\Gamma_1-\overline{\Gamma})\,\overline{\Gamma}/\Gamma_1+\overline{\Gamma}(1-\overline{\Gamma}/\Gamma_1)\\ &= \overline{\Gamma}(\Gamma_1-\overline{\Gamma})\end{aligned}$$

or

$$(1+\overline{\gamma^2}/\overline{\Gamma}^2)\,\overline{\Gamma}/\overline{\Gamma}_c = \Gamma_1/\overline{\Gamma}_c, \tag{10}$$

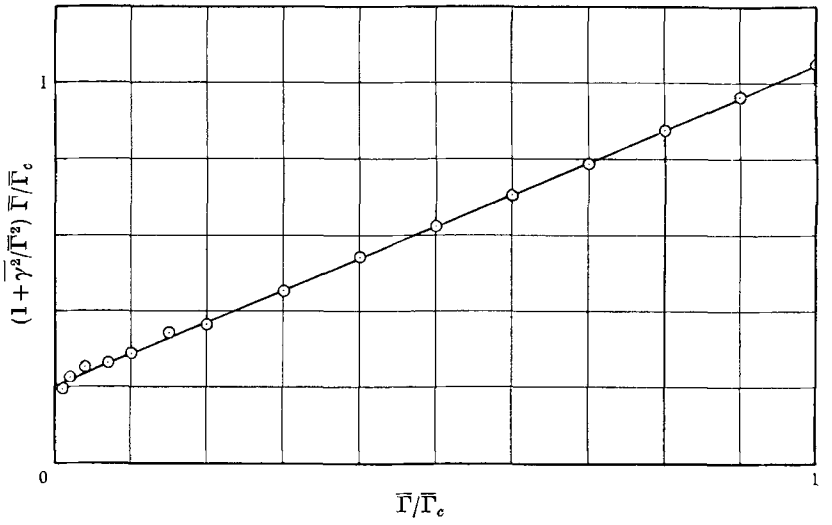


FIGURE 8. The relation between the concentration fluctuation intensity and the mean concentration.

where $\overline{\delta}$ is the intermittency factor—the fraction of time during which $\Gamma > 0$. Figure 8 accordingly shows the graph of $(1+\overline{\gamma^2}/\overline{\Gamma}^2)\,\overline{\Gamma}/\overline{\Gamma}_c$ *vs* $\overline{\Gamma}/\overline{\Gamma}_c$. The ordinate is clearly not independent of the abscissa, but since the model is obviously too simple a close correspondence is not expected. What is useful is that the relationship is linear and yields the highly accurate correlating equation

$$\overline{\gamma^2} = 0{\cdot}205\overline{\Gamma}\overline{\Gamma}_c - 0{\cdot}156\overline{\Gamma}^2. \tag{11}$$

## 6. Properties of the turbulent jet fluid

With knowledge of the concentration intermittency factor the properties of the turbulent jet fluid are easily estimated (Becker *et al.* 1965). The mean concentration is

$$\overline{\Gamma}_T = \overline{\Gamma}/\overline{\delta}. \tag{12}$$

The mean-square concentration fluctuation is

$$\overline{\gamma_T^2} = [\overline{\delta}\overline{\gamma^2}-(1-\overline{\delta})\,\overline{\Gamma}^2]/\overline{\delta}^2$$

or

$$\overline{\gamma_T^2}/\overline{\Gamma}_T^2 = \overline{\delta}\overline{\gamma^2}/\overline{\Gamma}^2-(1-\overline{\delta}). \tag{13}$$

The last relation, written as

$$\overline{\gamma^2} = \overline{\delta}\overline{\gamma_T^2}+\frac{1-\overline{\delta}}{\overline{\delta}}\,\overline{\Gamma}^2,$$

says that the total mean-square fluctuation $\overline{\gamma^2}$ is the sum of a term $\overline{\delta}\overline{\gamma_T^2}$ due to concentration fluctuations within the turbulent jet fluid and a term $(1-\overline{\delta})\,\overline{\Gamma}^2/\overline{\delta}$ due to intermittent pressure of the jet fluid.

The equilibrium values of $\overline{\Gamma}_T/\overline{\Gamma}_c$ and $\gamma'_T/\overline{\Gamma}_T \equiv \sqrt{(\overline{\gamma_T^2})}/\overline{\Gamma}_T$ computed from the above formulae are given in the last two columns of table 1. At the edge of the

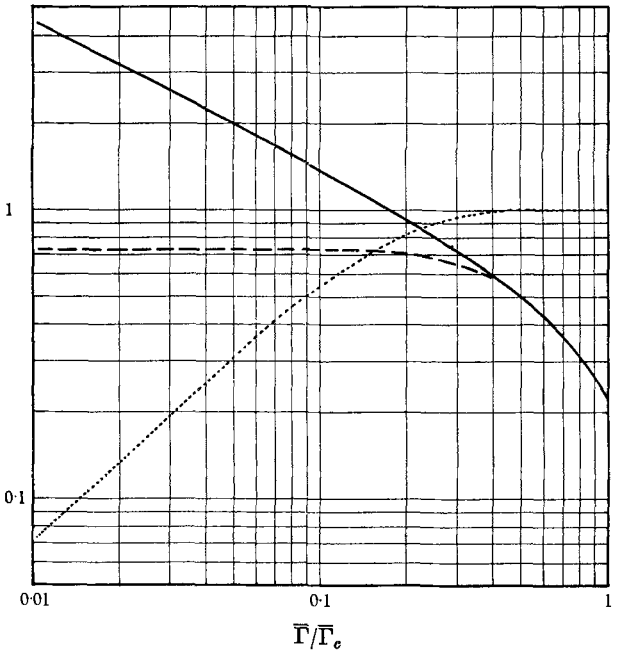


FIGURE 9. Properties of the jet as a function of the mean concentration level: ——, $\gamma'/\overline{\Gamma}$, the overall concentration fluctuation intensity; – – – –, $\gamma'_T/\overline{\Gamma}_T$, the relative concentration fluctuation intensity in the turbulent fluid; ·····, $\overline{\delta}$, the intermittency factor.

jet the value of $\overline{\Gamma}_T/\overline{\Gamma}_c$ is around 0·2, which agrees with (11) which predicts that at the edge $\Gamma_1 = 0{\cdot}205\overline{\Gamma}_c = \overline{\Gamma}_T$ on the assumption that the concentration fluctuations are produced purely by intermittency with $\Gamma$ fluctuating between zero and $\Gamma_1$.

Figure 9 shows the overall relative intensity $\gamma'/\overline{\Gamma}$ and the relative intensity within the jet fluid $\gamma'_T/\overline{\Gamma}_T$ as functions of $\overline{\Gamma}/\overline{\Gamma}_c$. In the greater part of the region of intermittency ($\overline{\Gamma} < 0{\cdot}2\overline{\Gamma}_c$) the relative intensity in the jet fluid is constant at about 0·73. At $\overline{\Gamma} < 0{\cdot}1\overline{\Gamma}_c$ the bulk of the overall fluctuation $\overline{\gamma^2}$ is clearly due to intermittency.

## 7. The one-dimensional spectrum of the concentration fluctuations

The concentration fluctuations were spectrally analyzed at points on the jet centre line. The spectral densities were corrected for random noise and limited spatial resolution (see I for details of these corrections) but a limit was always reached beyond which the signal was lost in noise.

The spectrum on the jet centre line becomes self-preserving in shape at about the same axial position as the mean concentration profile, $x = 40r_0$. Figure 10 shows the self-preserving form with the data for $x = 64r_0$ (the normalizing factor for the wave-number is the axial integral scale $\Lambda_\gamma$, discussed in § 8). At about $\kappa = 2/\Lambda_\gamma$ the decay of the spectral density with increasing wave-number settles into the $(-\frac{5}{3})$-power mode, figure 11. The equation of this region is

$$E(\Lambda_\gamma \kappa) = 0{\cdot}395(\Lambda_\gamma \kappa)^{-\frac{5}{3}}. \tag{14}$$

Meaningful data could not be obtained beyond about $\Lambda_\gamma \kappa = 50$, owing to random noise.

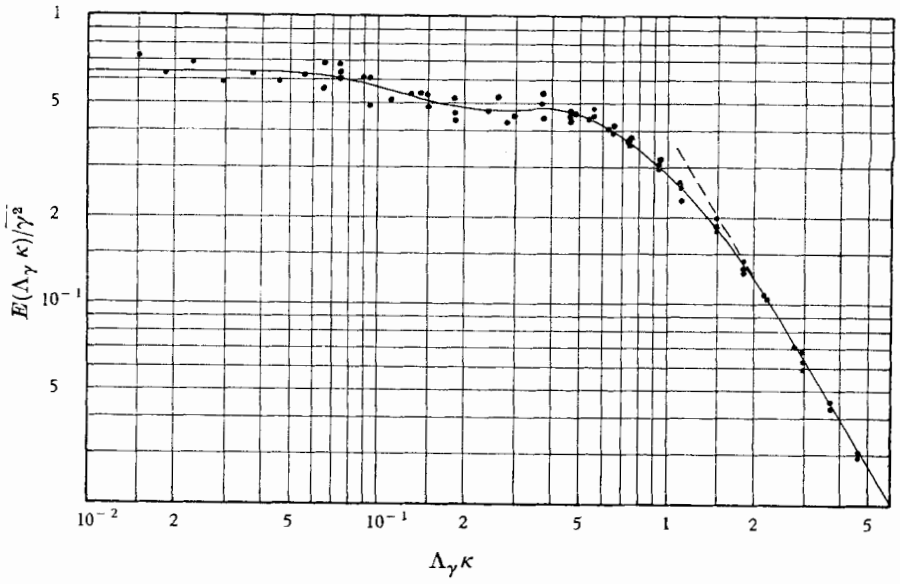


FIGURE 10. The concentration fluctuation spectrum on the jet centre line at $x = 64r_0$, at low wave-numbers.

A numerical specification of the self-preserving spectrum up to $\Lambda_\gamma \kappa = 0{\cdot}2$ is given in table 2. In the range $0{\cdot}6 < \Lambda_\gamma \kappa < 2{\cdot}2$ the spectral densities are given by the von Kármán-type interpolation formula

$$E(\Lambda_\gamma \kappa) = 0{\cdot}594[1 + 1{\cdot}455(\Lambda_\gamma \kappa)^2]^{-\frac{5}{6}}. \tag{15}$$

At $\Lambda_\gamma \kappa > 2{\cdot}2$ equation (14) applies. If a von Kármán formula applied at all wave-numbers it would be

$$E(\Lambda_\gamma \kappa) = (2/\pi)[1 + 1{\cdot}793(\Lambda_\gamma \kappa)^2]^{-\frac{5}{6}}. \tag{16}$$

At high wave-numbers this reduces to

$$E(\Lambda_\gamma \kappa) = 0{\cdot}392(\Lambda_\gamma \kappa)^{-\frac{5}{3}}, \tag{17}$$

which is virtually the same as (14).

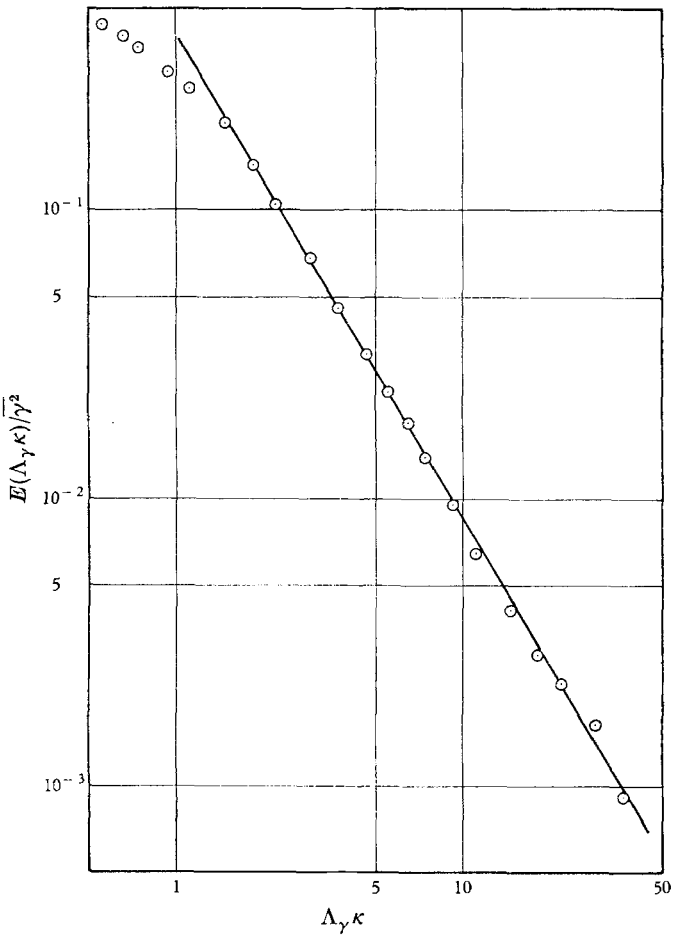


FIGURE 11. The concentration fluctuation spectrum on the jet centre line at $x = 64r_0$, in the equilibrium range of wave-numbers.

| $\Lambda_\gamma\kappa$ | $E(\Lambda_\gamma\kappa)$ | $\Lambda_\gamma\kappa$ | $E(\Lambda_\gamma\kappa)$ | $\Lambda_\gamma\kappa$ | $E(\Lambda_\gamma\kappa)$ |
|---|---|---|---|---|---|
| 0 | 0·638 | 0·2 | 0·485 | 0·7 | 0·381 |
| 0·05 | 0·638 | 0·25 | 0·480 | 1 | 0·281 |
| 0·07 | 0·638 | 0·3 | 0·480 | 1·5 | 0·178 |
| 0·1 | 0·583 | 0·4 | 0·480 | 2 | 0·121 |
| 0·15 | 0·510 | 0·5 | 0·458 | 2·5 | 0·086 |

TABLE 2. Numerical specification of the self-preserving one-dimensional spectrum of concentration fluctuations

## 8. The integral scale of concentration fluctuations

The axial integral spatial scale of the concentration fluctuations is defined by

$$\Lambda_\gamma \equiv \int_0^\infty C\,d\xi, \tag{18}$$

where $$C(x, r, \phi; x+\xi, r, \phi) \equiv \overline{\gamma_A \gamma_B}/\gamma'_A \gamma'_B$$

is the correlation coefficient between the fluctuations $\gamma_A \equiv \gamma(x, r, \phi)$ and $\gamma_B \equiv \gamma(x+\xi, r, \phi)$ at two points $A$ and $B$ an axial distance $\xi$ apart. If it is supposed that the turbulence pattern is translated past any point $(x, r, \phi)$ effectively frozen and moving at the local mean velocity $\overline{U}$ (a fair approximation on the jet centre line if not elsewhere), then the correlation function $Q(\xi) \equiv \overline{\gamma_A \gamma_B}$ is related to the one-dimensional spectral density function by the Fourier transformation

$$Q(\xi) = \int_0^\infty E(\kappa) \cos(\kappa\xi)\, d\kappa. \tag{19}$$

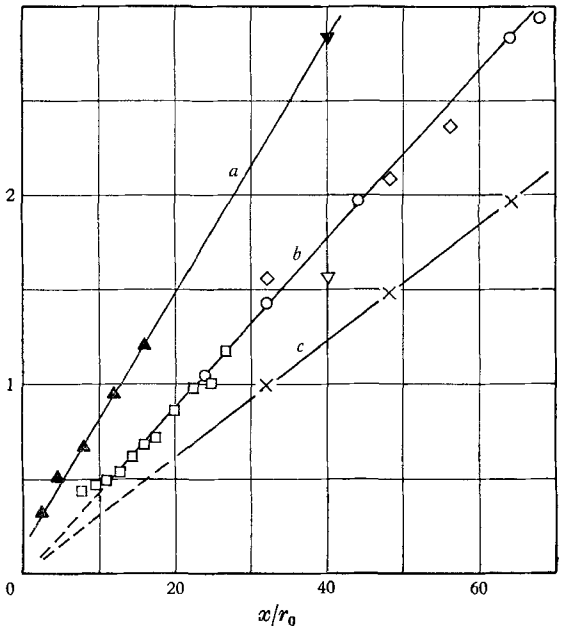


FIGURE 12. Integral spatial scales, normalised with respect to the nozzle radius $r_0$, as functions of axial position. ▲ ▼: $\Lambda_u/r_0$, axial scale of velocity fluctuations on the jet centre line; ○ □ ◇: $\Lambda_\gamma/r_0$, axial scale of concentration fluctuations on the jet centre line; ▽: axial scale of temperature fluctuations on the jet centre line; + : $\sigma/r_0$, 'wrinkle amplitude' of the jet boundary; ▲: Laurence (1956); ▽ ▼: Corrsin & Uberoi (1951); ○ □ ◇ + : present data. Mode of analysis: ○, bandpass filter (frequency analyser); □, 1200 c/s lowpass filter; ◇, 81 c/s lowpass filter.

It follows from the inverse transformation (see, e.g. Hinze 1959) that

$$\Lambda_\gamma = \tfrac{1}{2}\pi \overline{U} E(0)/\overline{\gamma^2}. \tag{20}$$

Two approaches were used in the present work to evaluate $\Lambda_\gamma$ by the above formula. In the first the entire spectrum was measured with a tuneable bandpass electronic filter (a sound and vibration analyzer) and $\Lambda_\gamma$ was evaluated from the intercept at zero wave-number. In the second a low-pass filter was used to obtain the fluctuation energy in a white-noise pass-band $(0, 0+\Delta f)$; then

$$\Lambda_\gamma = \tfrac{1}{4}\overline{U}\overline{\gamma^2_{0,\Delta f}}/\overline{\gamma^2}\,\Delta f, \tag{21}$$

when $\Delta f$ is sufficiently small. In all these measurements the usual corrections were made so that

$$\overline{\gamma^2} = \int_0^\infty E(\kappa)\, d\kappa$$

with $E(\kappa)$ following the $(-\frac{5}{3})$-power law at the higher wave-numbers right up to $\kappa = \infty$. Thus the values of $\Lambda_\gamma$ obtained are, like those of $\overline{\gamma^2}$, appropriate to a Schmidt number on the order of unity—the normal case in gas mixing.

The measured integral scales on the jet centre line are shown as a function of axial position in figure 12. The relation is essentially linear, following the equation

$$\Lambda_\gamma = 0{\cdot}0445x. \tag{22}$$

## 9. Correlation coefficient

The symmetrical lateral correlation coefficient,

$$C(x, \tfrac{1}{2}\xi, \phi; x, \tfrac{1}{2}\xi, \phi+\pi) \equiv \frac{\overline{\gamma(x, \frac{1}{2}\xi, \phi)\,\gamma(x, \frac{1}{2}\xi, \phi+\pi)}}{\overline{\gamma^2(x, \frac{1}{2}\xi, \phi)}}, \tag{23}$$

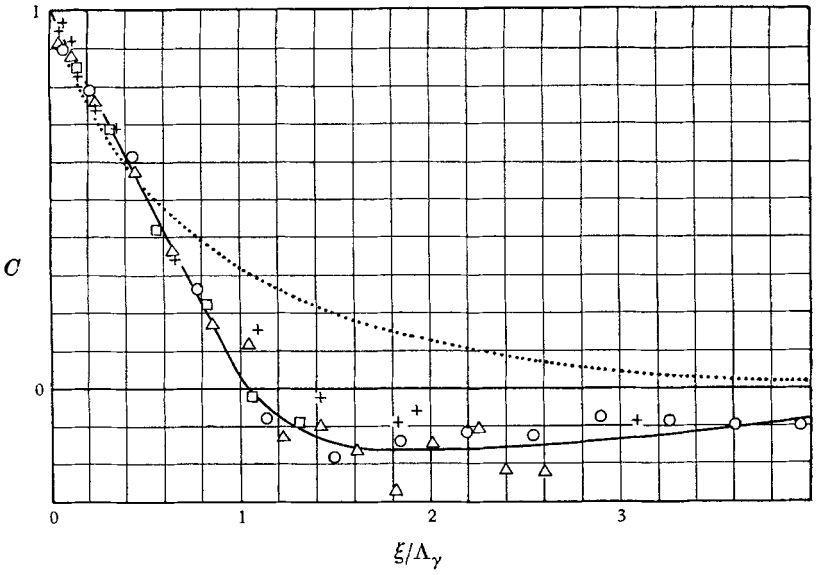


FIGURE 13. Correlation coefficients as functions of the separation distance. The dotted curve represents the axial correlation coefficient of concentration fluctuations on the jet centre line. The data points ○, □ and △ are the present data on the symmetrical lateral correlation coefficient of concentration fluctuations. The data points + are the data of Corrsin & Uberoi (1951) on the symmetrical lateral correlation coefficient of temperature fluctuations. Axial positions $x/r_0$ are: ○, 40; □, 56; △, 72; and +, 40.

was measured by detecting two segments of the same light beam through a double-slitted plate with two photocells and varying the centre-to-centre separation distance between the segments. The separation distance was corrected for the displacement effect on spatial resolution as described in I. Figure 13 shows this correlation coefficient as a function of the corrected and normalized separation distance, the normalizing scale being the integral scale $\Lambda_\gamma$.

The axial correlation coefficient on the jet centre line was computed from the self-preserving form of the one-dimensional spectrum—with the $(-\frac{5}{3})$-power law applying at high wave-numbers—by the Fourier transformation

$$C(x, r, \phi; x+\xi, r, \phi) = \frac{1}{\overline{\gamma^2}} \int_0^\infty E(\kappa) \cos(\kappa\xi)\, d\kappa,$$

a formula which follows from (19). The dotted curve in figure 13 shows this coefficient as a function of the normalized separation distance.

It should be remembered that the vertex behaviour of the curves in figure 13 is artificial: the parabolic region which should appear in the neighbourhood of zero separation distance is absent, due to an inherent limitation of the light-scatter technique, and the behaviour seen is appropriate to the non-existent case in which the $(-\frac{5}{3})$-power law extends to infinite wave-number. The error in the absolute value of the correlation coefficient near $\xi = 0$ is very small, however; it is rather the derivatives $dC/d\xi$ and $d^2C/d\xi^2$ which are wrong.

| | Jet | Scalar† | $C_1$ | $C_2$ | $C_3$ |
|---|---|---|---|---|---|
| Present data | Air/air | Concentration | 0·1060 | 0·0925 | 1·147 |
| Corrsin (1943) | Air/air | Temperature | 0·110 | 0·096 | 1·15 |
| Corrsin & Uberoi (1950) | Air/air | Temperature | 0·107 | 0·139 | 0·77 |
| Hinze & van der Hegge Zijnen (1949) | Air/air | Concentration and temperature | 0·096 | — | — |
| Keagy & Weller (1949) | $N_2$/air | Concentration | 0·105 | — | — |
| Ruden (1933) | Air/air | Temperature | 0·103 | 0·086 | 1·20 |
| Sunavala, Hulse & Thring (1957) | Gas/air | Concentration and temperature | 0·117 | 0·110 | 1·06 |
| Wilson & Danckwerts (1964) | Air/air | Temperature | 0·130 | 0·0875 | 1·49 |
| Forstall & Gaylord (1955) | Water/water | Concentration | 0·103 | — | — |
| Kizer (1963) | Water/water | Concentration | 0·104 | 0·100 | 1·04 |
| Kristmanson & Danckwerts (1961) | Water/water | Concentration | 0·112 | 0·105 | 1·06 |

† The results quoted for the temperature field are those for which the difference between the nozzle and ambient temperatures was under 20 °C.

TABLE 3. Constants in the laws of the mean scalar (concentration or temperature) field

## 10. Discussion

The mean concentration data can be compared with literature results in terms of the decay law of the centre line concentration and the growth law of the concentration half-radius. The standard forms of these laws are

$$b_{\frac{1}{2}} = C_1(x - x_0), \tag{24}$$

$$\Gamma_0/\bar{\Gamma}_c = C_2(x - x_0)/r_0. \tag{25}$$

It may also be observed that in consequence of the simultaneous conservation of axial momentum and nozzle fluid, in self-preservation

$$\bar{\Gamma}_c b_{\frac{1}{2}} = C_3 \Gamma_0 r_0, \tag{26}$$

where $C_3 = C_1/C_2$.

Table 3 compares the values found by different investigators for the constants $C_1$, $C_2$ and $C_3$. There is fairly good agreement on the radial jet growth constant $C_1$, but the values of the axial decay constant $C_2$ vary considerably. The results of Ruden (1933) and of Hinze van der Hegge Zijnen (1949) for $C_1$, of Corrsin & Uberoi (1950) for $C_2$, and of Wilson & Danckwerts (1964) for both $C_1$ and $C_2$ are

sufficiently atypical to suggest a possibility of error or exceptional boundary conditions. The constants $C_1$ and $C_2$ are both differential coefficients and require very accurate and complete primary data for their accurate evaluation. It appears that the data of Ruden and of Hinze & van der Hegge Zijnen did not extend far enough downstream to accurately define the properties of the equilibrium state. The results of Corrsin & Uberoi suggest that the abnormality of Wilson & Danckwerts value of $C_1$ may be due to the effects of high nozzle temperatures.

Literature data (references in table 3) on the self-preserving radial profile of a scalar property (concentration or temperature) passively marking the nozzle fluid of a turbulent round jet show considerably greater scatter than the data in figure 2, so much so that any systematic differences are masked and the only firm conclusion resulting is that there is generally good first-order agreement among different investigators. It appears that the present results, due to the advantages of the light scatter technique, are the first of sufficiently high quality to define with some accuracy such derivative quantities as the radial gradient of the mean concentration of the nozzle fluid.

Up to about $r/b_{\frac{1}{2}} = 1{\cdot}5$ the profile of the concentration fluctuation intensity normalized with respect to the centre line value, figure 5, is virtually the same as the corresponding temperature profile measured by Wilson & Danckwerts (1964) with a wire-probe resistance thermomenter. Beyond this point the temperature fluctuation intensity diminishes more rapidly with radial distance, perhaps because of inadequate response of the resistance wire thermometer to large-amplitude fluctuations (as in hot-wire anemometry).

The relative concentration fluctuation intensity on the jet centre line apparently tends to an equilibrium value of $\gamma'/\overline{\Gamma} = 0{\cdot}22$. Wilson & Danckwerts (1964) temperature data for a nozzle temperature of 225° C appear to level off at a relative intensity of 0·18. It is not clear now whether this difference is genuine (due to the difference in the Schmidt and Prandtl numbers), whether it is due to inadequate response of the wire resistance thermometer to such large fluctuation levels, or whether it is due to the density fluctuations accompanying temperature fluctuations.

The concentration fluctuation energy spectrum on the jet centre line, figures 10 and 11, compares closely in shape with the temperature fluctuation spectrum measured by Corrsin & Uberoi (1950). Both spectra exhibit a $(-\frac{5}{3})$-power law over at least two decades of wave-number variation. Gibson (1962, 1963) has determined that velocity fluctuations also exhibit this feature at high Reynolds numbers.

Corrsin & Uberoi (1951) made one measurement of the axial integral scale of temperature fluctuations on the jet centre line. This datum has been adjusted to the present experimental conditions by assuming that the ratio $\Lambda_\gamma/b_{\frac{1}{2}}$ for jet temperature fields is independent of the temperature difference between the nozzle fluid and the ambient fluid. The adjusted point is shown in figure 12. On the basis of this isolated piece of evidence, the spatial scales of concentration fluctuations and temperature fluctuations would appear to differ negligibly for Schmidt or Prandtl numbers around unity.

The axial scale of axial velocity fluctuations on the jet centre line in isothermal,

air/air, round free jets has been measured by Corrsin & Uberoi (1951) and Laurence (1956). These results are shown in figure 12, and are correlated by the equation

$$\Lambda_u/r_0 = 0{\cdot}068(x/r_0 + 1{\cdot}9). \tag{27}$$

Thus the ratio between the axial scales of the concentration or temperature fluctuations and the axial velocity fluctuations is $\Lambda_\gamma/\Lambda_u = 0{\cdot}66$.

Corrsin & Kistler (1955) studied intermittency by a hot-wire anemometer technique. They obtained jet radii $\bar{R}$ about 10 % smaller than the present values and wrinkle amplitudes $\sigma$ about 60 % larger. No good explanation for the large difference in $\sigma$ is immediately evident. However, it may be observed that the present light-scatter technique of detecting intermittency rests on a sharply defined and experimentally uncomplicated operation, whereas the detection of intermittency through velocity fluctuations is inherently more nebulous and experimentally difficult. The evidence indicates that the present measurements were highly accurate: the formation of the intermittency signal was monitored on a dual-trace oscilloscope and the effectiveness of the transformation was thus directly verified.

The correlation coefficients shown in figure 13 behave much as expected: the symmetrical lateral coefficient about equals the centre line axial coefficient at small separation distances and is smaller at large separation distances. Further, at large separation distances the lateral coefficient is quite strongly negative.

Corrsin & Uberoi (1951) measured the symmetrical lateral correlation coefficient for temperature fluctuations 40 nozzle radii from the nozzle mouth. These results are depicted by the crosses in figure 13 and correspond closely with the present data for concentration fluctuations.

It is interesting to compare the self-preserving values of the spatial scales. In terms of the mean jet radius $\bar{R}$

$$\sigma = 0{\cdot}161\bar{R}, \quad \Lambda_\gamma = 0{\cdot}236\bar{R}, \quad \Lambda_u = 0{\cdot}34\bar{R}, \quad b_{\frac{1}{2}} = 0{\cdot}56\bar{R}.$$

Denote the velocity half-radius by $r_{\frac{1}{2}}$,

$$r = r_{\frac{1}{2}} \quad \text{at} \quad \overline{U} = \tfrac{1}{2}\overline{U}_c.$$

The results of most investigators give

$$r_{\frac{1}{2}} = (0{\cdot}085 \pm 0{\cdot}002)\,(x - x_0).$$

Thus in self-preservation

$$r_{\frac{1}{2}} = 0{\cdot}45\bar{R}.$$

Now the wrinkle amplitude $\sigma$ is a measure of the average eddy size in the radial direction. The fact that $\sigma$ is smaller than either of the integral scales $\Lambda_\gamma$ and $\Lambda_u$ therefore suggests that the large eddies are elongated in the axial direction.

The integral scales $\Lambda_\gamma$ and $\Lambda_u$ are large, about $\frac{1}{4}$ and $\frac{1}{3}$ of the mean jet radius $\bar{R}$. In a pipe flow the integral scales are relatively small, around $\frac{1}{12}$ of the pipe radius (see Becker, Rosensweig & Gwozdz 1966). Thus the assumption in many of the classical theories of the mean velocity, concentration, and temperature fields in turbulent shear flows, namely that the turbulence scale is small relative to the lateral scale of the field, is unreal for jets.

## 11. Conclusion

The light-scatter technique has evidently yielded a very accurate description of the nozzle-fluid concentration field of the round, turbulent free jet. Comparison with the results of other investigators who used heat to mark the nozzle fluid indicates a close similarity between the concentration and temperature fields. The similarity disappears, however, when the spectrum at wave-numbers beyond the $(-\frac{5}{3})$-power (or equivalent) regime is important to the argument in hand.

An equally accurate study of the velocity field is needed now to facilitate a quantitative interpretation of the transport processes in the jet.

This work was supported by the U.S. Army Research Office (Durham); Grant No. DA-ARO(D)-31-124-G8 and Project No. 2013-E.

REFERENCES

BECKER, H. A. 1961 Concentration fluctuations in ducted jet mixing. *Sci. D. dissertation, Mass. Inst. Tech.*

BECKER, H. A., HOTTEL, H. C. & WILLIAMS, G. C. 1963 *Ninth Symposium (International) on Combustion*, p. 7.

BECKER, H. A., HOTTEL, H. C. & WILLIAMS, G. C. 1965 *Tenth Symposium (International) on Combustion*, p. 1253.

BECKER, H. A., HOTTEL, H. C. & WILLIAMS, G. C. 1967 *J. Fluid Mech.* **30**, 259.

BECKER, H. A., ROSENSWEIG, R. E. & GWOZDZ, J. R. 1963 Turbulent dispersion in a pipe flow. *Air Force Cambridge Research Laboratories Rept.* no. *AFC RL*-63-727. Bedford, Mass.

BECKER, H. A., ROSENSWEIG, R. E. & GWOZDZ, J. R. 1966 *A.I.Ch.E. J.* **12**, 964.

CORRSIN, S. 1943 *NACA Wartime Rept.* no. W-94.

CORRSIN, S. & KISTLER, A. L. 1955 *NACA Rept.* no. 1244.

CORRSIN, S. & UBEROI, M. S. 1950 *NACA Rept.* no. 998.

CORRSIN, S. & UBEROI, M. S. 1951 *NACA Rept. no.* 1040.

FORSTALL, W. & GAYLORD, E. W. 1955 *J. Appl. Mech.* **22**, 161.

GIBSON, M. M. 1962 *Nature, Lond.* **195**, 1281.

GIBSON, M. M. 1963 *J. Fluid Mech.* **15**, 161.

HINZE, J. O. 1959 *Turbulence.* New York: McGraw-Hill Book Co. Inc.

HINZE, J. O. & VAN DER HEGGE ZIJNEN, B. G. 1949 *Appl. Sci. Res., Hague* A **1**, 435.

KEAGY, W. R. & WELLER, A. E. 1949 *Heat Transfer and Fluid Mechanics Institute*, p. 89. Berkeley, California.

KIZER, K. M. 1963 *A.I.Ch.E.J.* **9**, 386.

KRISTMANSON, D. & DANCKWERTS, P. V. 1961 *Chem. Engng Sci.* **16**, 267.

LAURENCE, J. C. 1956 *NACA Rept.* no. 1292.

ROSENSWEIG, R. E. 1959 Measurement and characterization of turbulent mixing. *Sci. D. dissertation, Mass. Inst. Tech.*

ROSENSWEIG, R. E., HOTTEL, H. C. & WILLIAMS, G. C. 1961 *Chem. Engng Sci.* **15**, 111.

RUDEN, P. 1933 *Naturwissenschaften*, **21**, 375.

SUNAVALA, P. D., HULSE, C. & THRING, M. W. 1957 *Combust. Flame*, **1**, 179.

WILSON, R. A. M. & DANCKWERTS, P. V. 1964 *Chem. Engng Sci.* **19**, 885.